日本原子力研究開発機構機関リポジトリ
Japan Atomic Energy Agency Institutional Repository

Title	Evaluation of the effects of differences in building models on the seismic response of a nuclear power plant structure
Author(s)	Choi B.,Nishida Akemi,Muramatsu Ken,Takada Tsuyoshi
Citation	Nippon Jishin Kogakkai Rombunshu,20(2),p.2_1-2_16
Text Version	Accepted Manuscript
URL	https://jopss.jaea.go.jp/search/servlet/search?5062640
DOI	https://doi.org/10.5610/jaee.20.2_1
Right	日本地震工学会

Japan Atomic Energy Agency

EVALUATION OF THE EFFECTS OF DIFFERENCES IN BUILDING MODELS ON THE SEISMIC RESPONSE OF A NUCLEAR POWER PLANT STRUCTURE

Byunghyun CHOI[1], Akemi NISHIDA[2], Ken MURAMATSU[3], and Tsuyoshi TAKADA[4]

[1] Researcher, Nuclear Safety Research Center, Japan Atomic Energy Agency, Japan, choi.byunghyun@jaea.go.jp
[2] Member of JAEE, Principal Researcher, Nuclear Safety Research Center, Japan Atomic Energy Agency, Japan, nishida.akemi@jaea.go.jp
[3] Member of JAEE, Visiting Professor, Department of Nuclear Safety Engineering, Tokyo City University, Tokyo, Japan, kmuramat@tcu.ac.jp
[4] Member of JAEE, Professor, Department of Architecture, The University of Tokyo, Tokyo, Japan, takada@load.arch.t.u-tokyo.ac.jp

ABSTRACT: This study examines two different seismic response analysis models of a nuclear power plant building, including the three-dimensional finite-element (3D FE) model with shell elements and the conventional sway-rocking model. Further, the results obtained using these models are compared for estimating the effects related with the differences between the modeling methods. In addition, the authors analyzed the spatial variations of the response results based on the merits of the 3D FE model, and the potential applications of this information are discussed.

Key Words: SPRA; NPP; Seismic response analysis; Uncertainty evaluation

1. INTRODUCTION

Since the 2011 Fukushima accident, nuclear power plants (NPPs) are required to establish countermeasures against ground motion beyond the seismic design basis. Also, the importance of seismic probabilistic risk assessment (SPRA) has drawn considerable attention. According to the procedural standard for SPRA of NPPs (Atomic Energy Society of Japan[1)] and Takada et.al[2)]), uncertainty can be classified as aleatory uncertainty (which originates from the inherent randomness and cannot be reduced) and epistemic uncertainty (which originates from the lack of knowledge and can be reduced using additional knowledge and/or information). Further, efforts should be made to identify and reduce the epistemic uncertainty caused by the lack of knowledge, if possible, for improving the reliability of SPRA. However, epistemic uncertainty has neither been well recognized nor properly quantified because of its estimation difficulty. Herein, the authors conducted seismic response analysis using two kinds of modeling methods (a three-dimensional finite-element (3D FE) model and a conventional lumped mass with sway-rocking (SR) model (SR model)), which addresses the epistemic uncertainty, and using various simulated input ground motions, which addresses the aleatory uncertainty. In the current SPRA, the coefficient method or partial modeling method based on the SR model is mainly

used for response evaluation of equipment and piping, but more realistic response evaluation using the 3D FE model is required. Further, the response results observed in case of different modeling methods were observed and statistically studied for quantifying the epistemic uncertainty.

2. ANALYSIS CONDITIONS

2.1 Hazard-Consistent Ground Motions

Ground motion is generated for Oarai, Japan (Latitude: 36.26°N; Longitude: 140.55°E), where the target NPP is located. Figure 1 depicts the site location, and Fig. 2 depicts the seismic hazard curve for the peak ground acceleration (PGA) defined at the free rock surface. Further, the seismic hazard is evaluated according to the method used at the Headquarters for Earthquake Research Promotion[3)], where the ground motion intensity was measured as the peak acceleration on a free rock surface. The attenuation relation proposed by Si and Midorikawa[4)] is adopted with a variation of 0.58, defined as the natural logarithm standard deviation. In this study, the target range of the ground motion reproduction is selected based on a previously conducted study (Nishida et al.[5)]). The target annual exceedance probability of ground motions is 10^{-4}–10^{-5}, corresponding to a PGA of 700–1100 cm/s^2 at the plant site. This PGA range is divided into four intervals of 100 cm/s^2 each, and 50 ground motions are generated in each interval, resulting in the production of a total of 200 ground motions within this range. The seismic sources generating these motions were selected according to their contributions to the site hazard based on a stochastic fault–rupture model, obtained by the disaggregation of the seismic hazard curve (Nishida et al.[5)]).

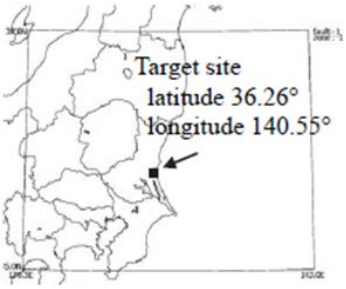

Fig. 1 Location of the target site (Nishida et al.[5)])

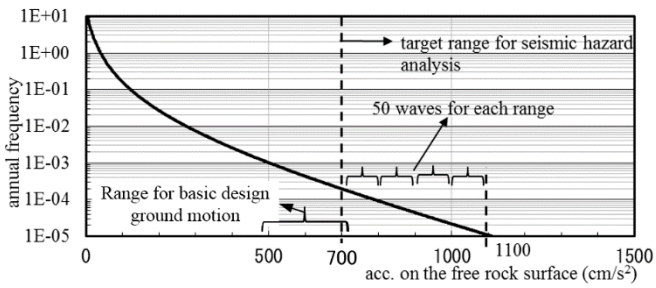

Fig. 2 Seismic hazard curve at the target site (Nishida et al.[5)])

Figure 3 denotes examples of the response spectra, whereas Fig. 4 denotes the acceleration time-history waveforms generated from different seismic sources. The shapes of the response spectra are observed to be quite different, and the response spectra variation in the horizontal (E–W and N–S) directions is smaller when compared with that in the vertical (U–D) direction. Also, regardless of the input ground motions, the hazard level remains the same (1000–1100 cm/s^2, E–W direction); however, the arrival time and duration are diverse. The examples demonstrate that the acceleration waveforms exhibit advantages over conventional PRA[1)] by which the shape of the input seismic motion spectrum is assumed to be the same as the uniform hazard spectrum or the NPP design basis earthquake without considering the variability of the spectrum.

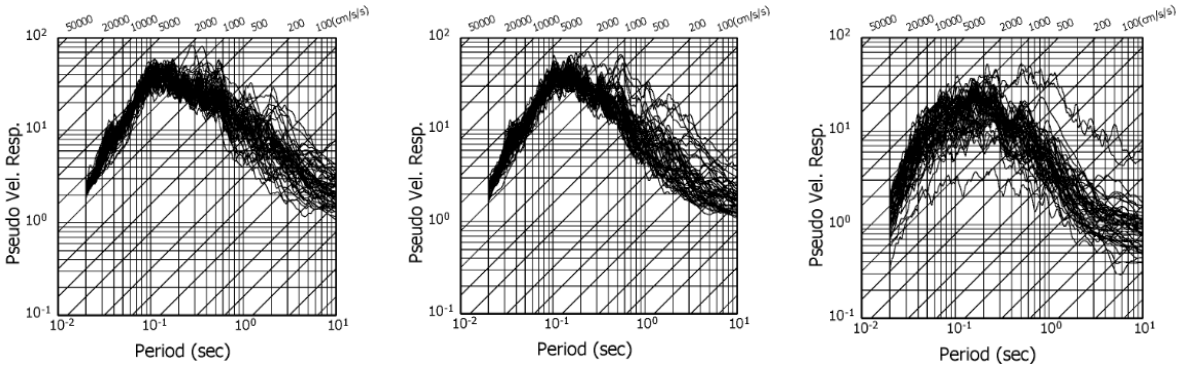

(a) E–W direction (b) N–S direction (c) U–D direction

Fig. 3 Response spectra of the generated input ground motions (700–800 cm/s^2) (Nishida et al.[5])

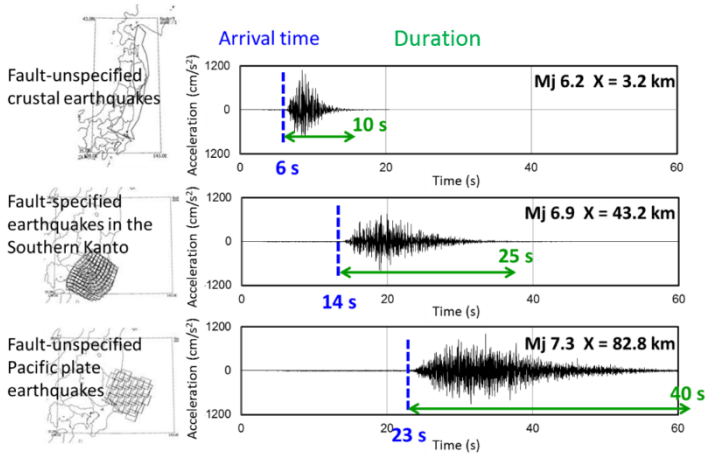

Fig. 4 Time-history waveforms of the generated input ground motions (1000–1100 cm/s^2, E–W direction) (Nishida et al.[5])

2.2 Analytical Models and Conditions

The NPP reactor building was modeled (i) as a 3D FE model containing shell elements and (ii) as a conventional lumped mass with an SR model. Further, the differences between the seismic responses of the two models will be quantified. Choi et al.[6), 7)] constructed a 3D FE model that mainly used shell elements for the walls and slabs and solid elements for the base mat, as depicted in Fig. 5(a). Here, the modeling of the equipment is considered as weight.

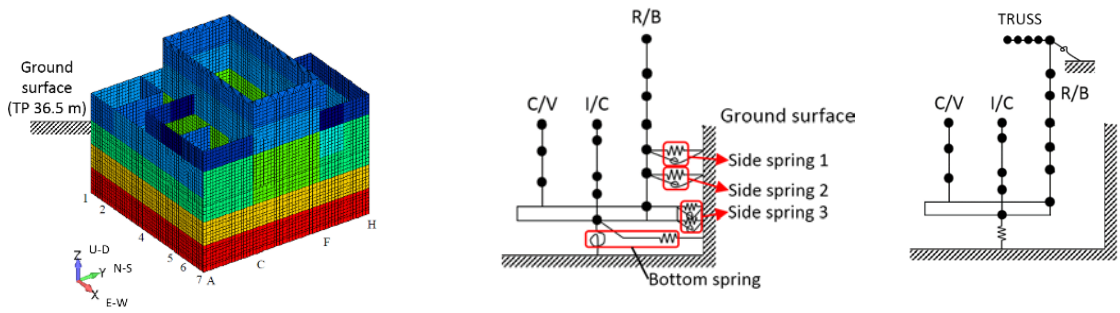

(a) 3D FE model (b) SR model (left: horizontal, right: vertical)

Fig. 5 Overview of the analytical models

There are approximately 50,000 nodes and approximately 60,000 elements. Further, the length of one side of the model mesh is approximately 1 m.

The constitutive model of reinforced concrete proposed by Maekawa (Maekawa et al.[8]) was considered for the seismic wall. The material properties (ignoring the rebar bond strength) are presented in Tables 1 and 2.

Table 1 Material properties of concrete

Compressive strength (kN/m^2)	Tensile strength (kN/m^2)	Strain at peak stress	Poisson's ratio	Damping ratio (h)
2.35×10^4	1.88×10^3	0.002	0.2	0.03

Table 2 Material properties of rebar

Young's modulus (kN/m^2)	Yield stress (kN/m^2)	Poisson's ratio	Damping ratio (h)
2.05×10^8	3.45×10^5	0.3	0.02

Half of the NPP building is embedded in the ground. The soil–structure interaction (SSI) is expressed with respect to the Winkler-type soil springs (Fig. 6). The spring value is based on the SR model (Nishida et al.[9]) and distributed at the nodes by dividing with the dominant area.

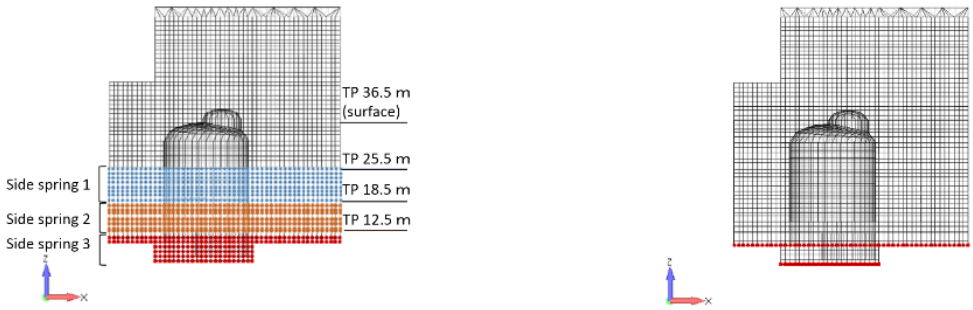

(a) Side springs (b) Bottom springs

Fig. 6. Attachment locations of soil springs (3D FE model) (Choi et al.[7])

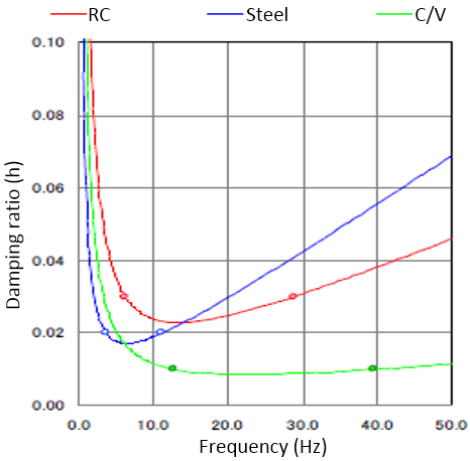

	Frequency (Hz)		Damping ratio	
	$f1$	$f2$	$h1$	$h2$
RC	6.19	28.81	0.03	0.03
Steel	3.61	11.13	0.02	0.02
C/V	12.73	39.52	0.01	0.01

(C/V: Containment vessel)

Fig. 7. Rayleigh damping

Seismic response analyses using 200 hazard-consistent ground-motion (HCGM) waves are generated by excitation in three directions (two horizontal-direction inputs and simultaneous vertical input).

Time-history response analysis is performed using Rayleigh damping h = 0.03 (RC), 0.02 (Steel), 0.01 (Containment Vessel, C/V) (Fig. 7) and direct time-integration methods based on the Newmark β method (β = 1/4 and γ =1/2). Further, the integration time interval Δt was 0.005 s.

2.3 Result of Eigenvalue Analysis for Model Verification

To verify the constructed 3D FE model, the authors compared the analytical results with the observational data. First, using one-dimensional wave propagation theory, the input wave were calculated in order to match the observation records and response results on the base mat. The acceleration response input wave spectra (Fig. 8) were provided as input below the base mat (Tokyo Peil (TP): 10 m). The installation positions of the seismographs (Choi et al.[10]) are depicted in Fig. 9, and the observed and analytical acceleration response spectra are presented in Fig. 10. These results denote that the observed and analytical results roughly matched with each other.

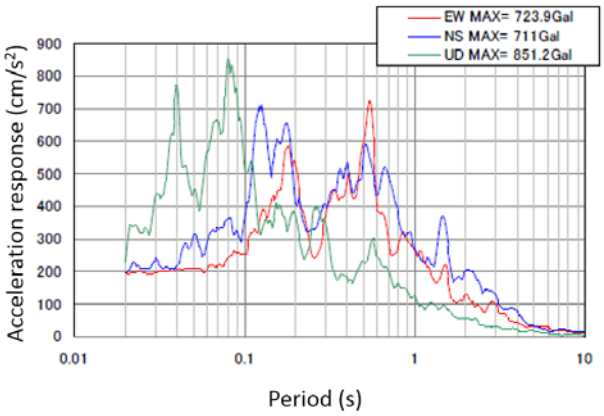

Fig. 8 Acceleration response spectra of the input wave (h = 5%)

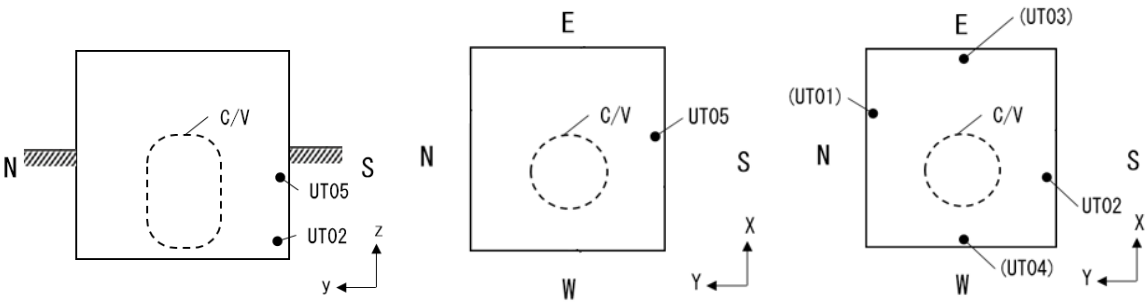

(a) Vertical section view (b) Plan view (B1F) (c) Plan view (B3F)

Fig. 9 Installation positions of seismographs

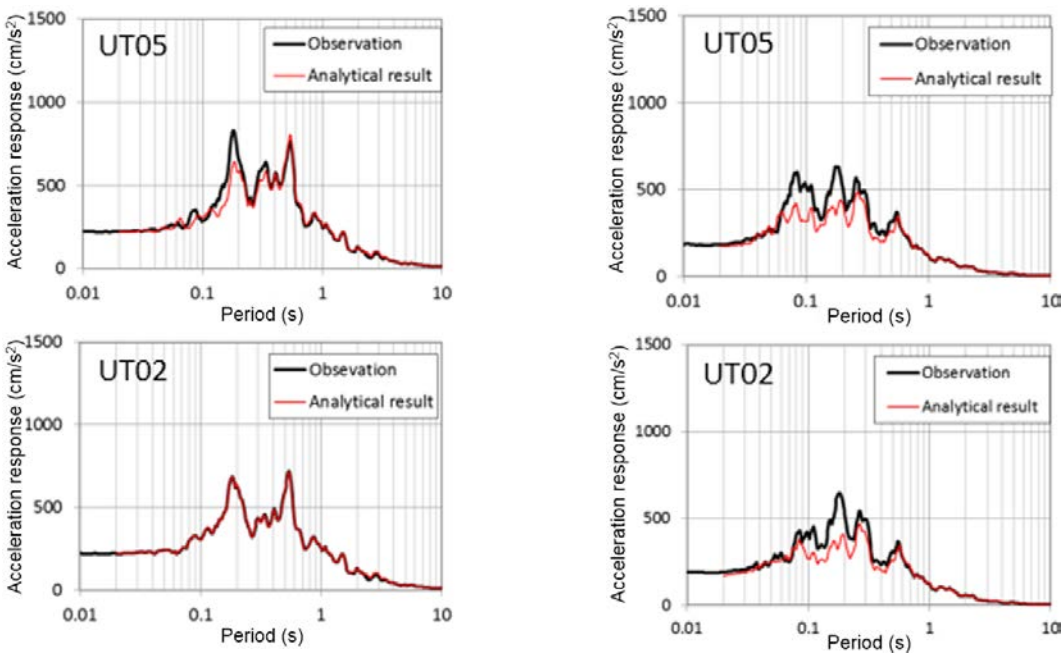

(a) EW direction

(b) UD direction

Fig. 10 Comparison of the observed data and analytical results (3D FE model)

Next, eigenvalue analyses were conducted using a fixed-base model and a soil–spring model. The results obtained from the 3D FE and SR models are presented in Table 3, and the first and second natural modes in the N–S direction are depicted in Figs. 11 and 12. According to the result of the fixed-base model, the natural period of the first mode of building was ~0.17 s, whereas that of the second mode was ~0.08 s. The first and second natural periods in each model correspond to each other. Further, based on the results of the soil–spring model, the natural period of the first mode was ~0.3 s, whereas that of the second mode was ~0.17 s. Again, the natural periods in each model correspond with each other. Further, the second mode of the soil–spring model corresponds to the first mode of the fixed–base model. Focusing on the second mode of the soil–spring model (0.17 s) shape in the 3D FE model (Fig. 12(c)) confirms the out-of-plane deformation in the upper part of the building, which could not be expressed using the SR model. This out-of-plane deformation mode is expected to affect the response of the upper part of the building by the 3D FE model. Similar results were obtained in the E–W direction.

Table 3 Eigenvalue analyses results for the reactor building model

Model	Mode	Fixed–base				Soil–spring			
		3D FE		SR		3D FE		SR	
		Freq. (Hz)	Period (s)	Freq. (Hz)	Period (s)	Freq. (Hz)	Period (s)	Freq. (Hz)	Period (s)
North–south (N–S)	1st	5.7	0.17	6.2	0.16	3.2	0.31	3.4	0.29
	2nd	11.8	0.08	11.4	0.09	5.7	0.17	6.5	0.15
East–west (E–W)	1st	6.4	0.15	6.2	0.16	3.2	0.32	3.4	0.29
	2nd	12.8	0.08	13.3	0.07	6.0	0.17	6.6	0.15

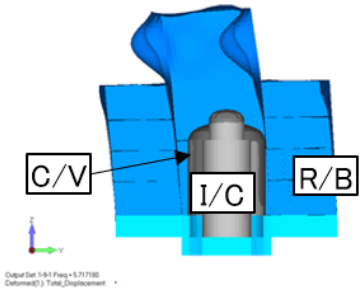

(a) First mode of 3D FE model (0.17 s)

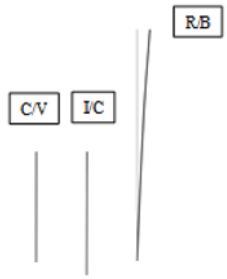

(b) First mode of SR model (0.16 s)

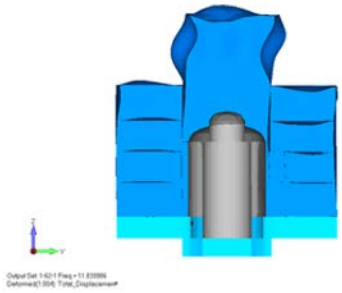

(c) Second mode of 3D FE model (0.08 s)

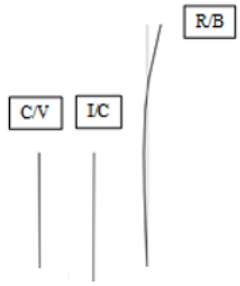

(d) Second mode of SR model (0.09 s)

Fig. 11 Mode shape obtained by the eigenvalue analyses with fixed–base model (N–S dir.)

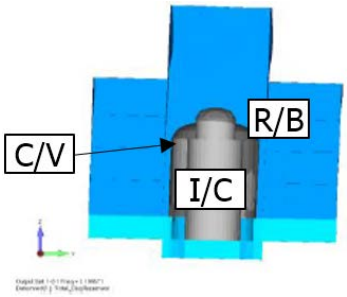

(a) First mode of 3D FE model (0.31 s)

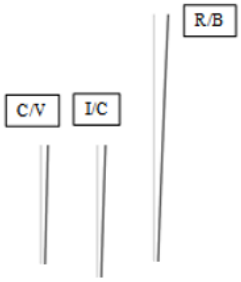

(b) First mode of SR model (0.29 s)

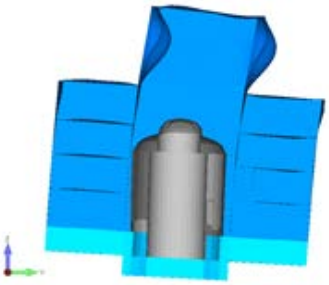

(c) Second mode of 3D FE model (0.17 s)

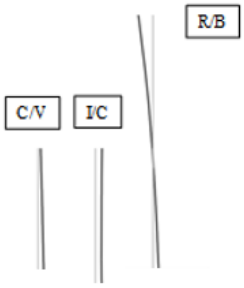

(d) Second mode of SR model (0.15 s)

Fig. 12 Mode shape obtained by eigenvalue analyses with the soil–spring model (N–S dir.)

3. ANALYTICAL RESULTS OF THE SHEAR WALL OF A REACTOR BUILDING

3.1 Maximum Acceleration Response Along the Height

The analytical results obtained using 200 ground motions were compared on a model-by-model basis. The maximum acceleration responses in the in-plane direction of the reactor building walls (4-A and 4-C line walls in Fig. 13) were compared. Initially, the maximum acceleration response distributions of

the 4-A line wall along the elevations per vertical datum TP were focused. Figure 14(a) depicts the analytical results of the maximum acceleration responses in the E–W direction of the 3D FE model based on 200 ground motions, and Fig. 14(b) depicts the average response of the 3D FE model (as the red line) and the SR model (as the black line) along the building height. Comparison of the average response confirmed the differences between the seismic responses of the two models for the upper part of the building. The maximum response ratio (3D FE/SR) was approximately 1.3 at a TP of 50.7 m. Because the operation floor above TP 50.7 m is a large space with few walls and columns, also the wall thickness becomes thinner in the upper floors, the out-of-plane deformation of the top floor is likely to occur; further, the wall perpendicular to the deformed wall is pulled by out-of-plane deformation; therefore, the maximum acceleration increased. The merit of using 3D FE model is that it can consider out-of-plane deformation. The difference was confirmed in the middle part of the building. This is assumed to be due to the difference in the method of modeling the SSI effects. Figure 14(c) shows the natural logarithm standard deviation due to the simulated ground motions in each model. Accordingly, the deviations in the 3D FE model are almost constant (~0.18) regardless of the height difference. However, the variations (~0.2) in the SR model are larger when compared with those in the 3D FE model, particularly in the middle part of the building. In addition, the difference in variations between the two models was the largest at a TP of 29.7 m, and its response ratio was 0.8.

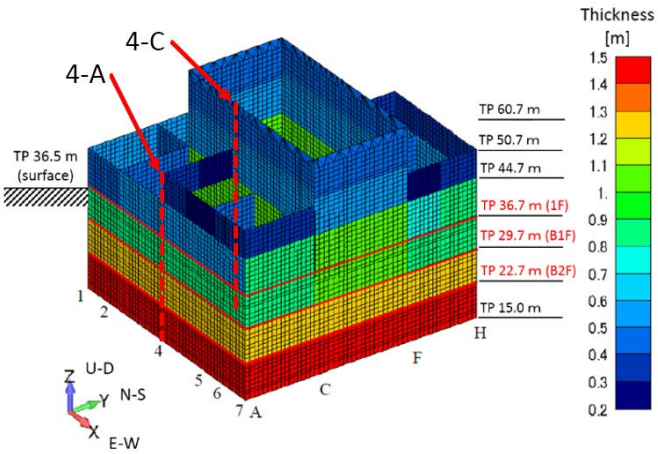

Fig. 13 Target reactor building (3D FE)

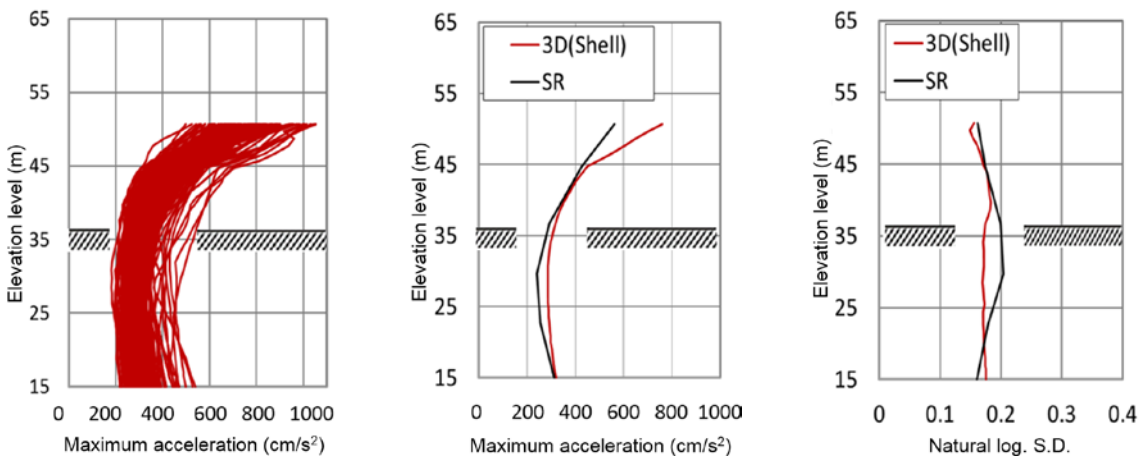

(a) Maximum acceleration response (b) Average (c) Natural logarithm standard deviation

Fig. 14 Statistics of maximum acceleration response (4-line wall, E–W direction)

3.2 Factor of Response Variations

In the conventional lumped mass SR model, it is impossible to consider the variation due to the difference in position within the same floor because there is only one evaluation point on each floor. The authors studied the variation due to the position difference to be used in the SR model based on the result of the 3D FE model. First, it was assumed that the total variations (β_T) of the two walls (4-A and 4-C line walls) obtained by the seismic response analysis results using a 3D FE model contained variations caused by the differences in ground motions and wall, which can be referred to as the variation due to the ground motions (β_g) and the due to the difference of the position (β_p), respectively. β_g indicates deviation from the average value of the maximum response of the wall at the same floor between 200 ground motions, whereas β_p indicates the difference between the deviations of maximum responses of the two walls at the same floor from each ground motion. This relation is expressed as

$$\beta_T = \sqrt{{\beta_g}^2 + {\beta_p}^2}. \tag{1}$$

The variations of the maximum acceleration response in the E–W direction of the 3D FE model are presented in Fig. 15. The horizontal axis denotes the natural logarithm standard deviation value. Accordingly, β_g of the 3D FE model is almost constant regardless of the building height, and the logarithm standard deviation values are ~0.18. Also, the influence of the variation of the between ground motions was larger than the variation in the ground motion. For reference, the variations of the SR model are denoted as a black dotted line in Fig. 15; its values are ~0.20 or less. Furthermore, β_p tends to increase with the building height, and the maximum logarithm standard deviation values are ~0.07 or less. Therefore, the authors propose a maximum of 0.07 for β_p while using the SR model.

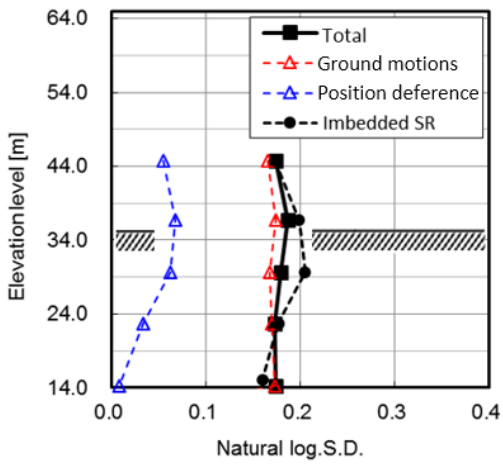

Fig. 15 Factor of response variations (E–W dir.) (Choi et al.[6])

4. ANALYTICAL RESULTS FOR THE FLOOR OF A REACTOR BUILDING

4.1 Maximum Acceleration Response of Reactor Building

Next, the difference in variations in the reactor building responses due to the modeling methods was investigated. The target building floors and details in the 3D FE model rendering are depicted in Figs. 13 and 16, respectively. The color indicates the thickness of each element in meters. The elevations of the three target floors, B2F, B1F, and 1F, are 22.7, 29.7, and 36.7 m, respectively. For reference, the ground surface is a TP of 36.5 m. Further, each floor is divided into four zones, as depicted in Fig. 16. (Zone 1 (red): North side, Zone 2 (blue): west side, Zone 3 (green): south side, Zone 4 (yellow): east side) The average values of the maximum acceleration response in the N–S direction for each zone were calculated and expressed along the X-axis (E–W direction).

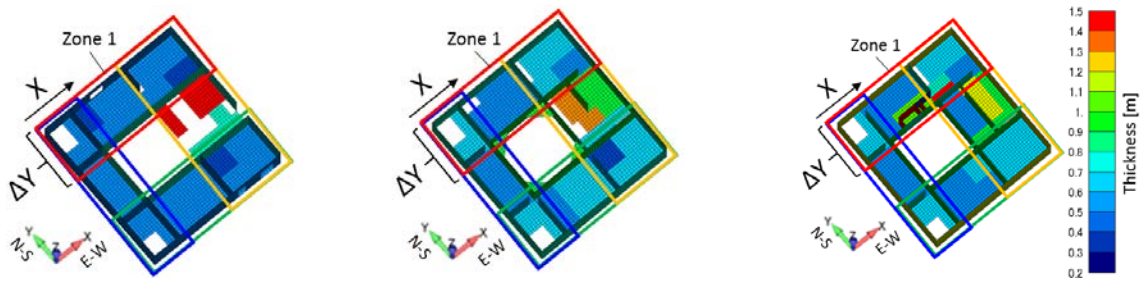

(a) 1F (TP 36.7 m) (b) B1F (TP 29.7 m) (c) B2F (TP 22.7 m)

Fig. 16 Detail of the target floors (3D FE)

For example, the median and variation (natural logarithm standard deviation) of the floor maximum acceleration response for the first floor (TP 36.7 m) based on 50 HCGMs of 700–800 cm/s^2 are denoted in Fig. 17. Here, although the results of the SR model are constant at the same height, they are indicated by a line for performing comparison with a 3D FE model. Also, the authors compared the mean and median for obtaining the average; as the result they denoted almost the same trend, the authors have used the median in this study.

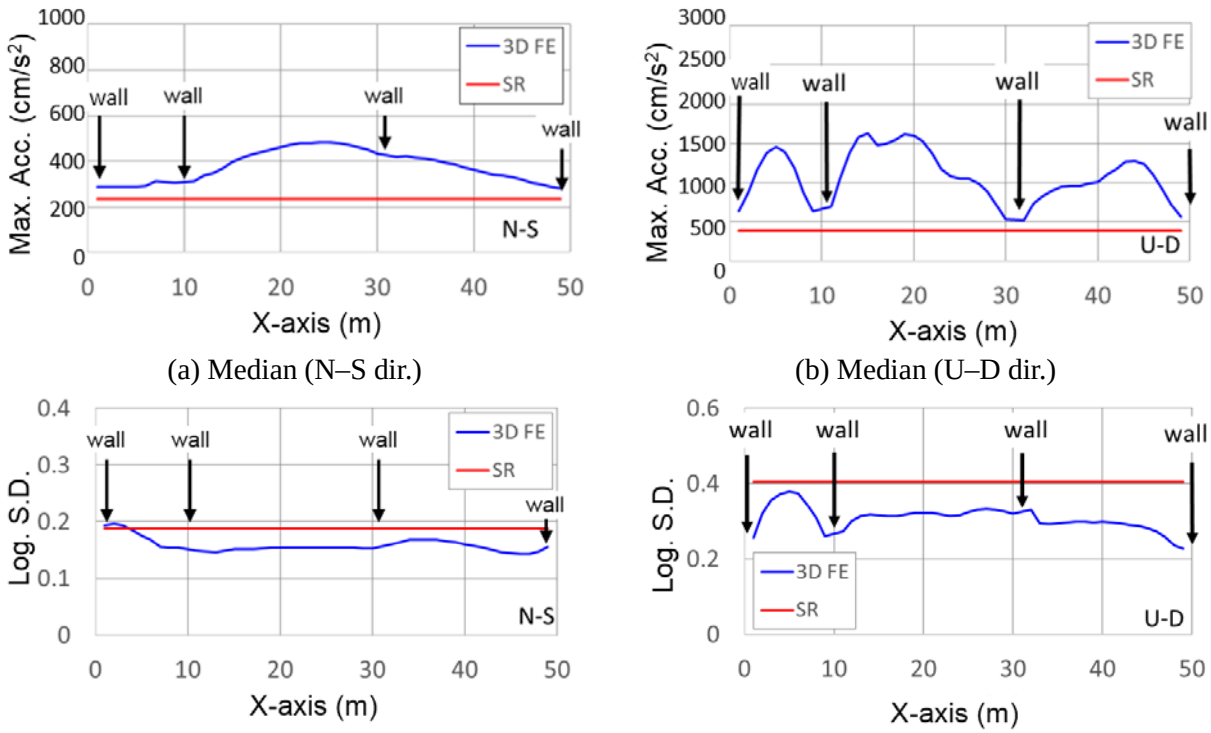

(a) Median (N–S dir.) (b) Median (U–D dir.)

(c) Natural logarithm standard deviation (N–S dir.) (d) Natural logarithm standard deviation (U–D dir.)

Fig. 17 Comparison of the statistical results due to modeling methods (1F, Zone 1 (3D FE), 700–800 cm/s^2)

According to Fig. 17(a), which is the median result of the 3D FE model obtained in the N–S direction; the result in the central part is larger than that at either end of the floor. Further, the median result of the SR model was smaller than the result of the 3D FE model. The response ratio (3D FE/SR) with respect to the 1F of the N–S direction was ~1.6. According to Fig. 17(b), in the U–D direction, the response results of the 3D FE model were small at 0, 10, 31, and 49 m along the X-axis, where the shear wall was located; the maximum values were observed at the midpoints between each of the shear wall locations. Because the analysis result had not denoted a strong nonlinear behavior, it can be assumed that the vertical motion was suppressed by the position of the shear wall. Also, in the U–D direction, the

median result from the SR model was smaller than that obtained from the 3D FE model. The response ratio on the 1F of the U–D direction was ~2.5.

According to Fig. 17(c), the variation in the N–S direction was about 0.1–0.2, which was smaller than the corresponding value of about 0.2–0.4 in the U–D direction (Fig. 17(d)). The ratio of the variation (3D FE/SR) at 1F was ~0.9 in the N–S direction and that of U–D direction was ~0.8. Also, in the U–D direction, the maximum variation could be observed around the 5-m position on the X-axis. This was presumed to be due to the influence of the opening in the floor depicted in Fig. 16(a). In addition, regardless of the direction, the variation in the SR model was larger than that in the 3D FE model. This is assumed to be due to the difference in the method of modeling the SSI effects. Based on the aforementioned comparison, various differences could be observed between the response results of the two modeling methods. It was possible to estimate the 3D effects, which cannot be completely expressed using the conventional SR model, using the 3D FE model.

4.2 Comparison Based on the Input Level

To confirm the effects of the changing input level, the response variation due to the increase in the input level was obtained. The median and the natural logarithm standard deviation of the maximum acceleration response of the HCGM input levels in 700–800, 800–900, 900–1000, and 1000–1100 cm/s^2 are compared in Figs. 18 and 19 respectively. The target floor of the 3D FE model was Zone 1 of the first floor (similar to that in the previous section). According to the results in the N–S direction, the median of the maximum acceleration increased as the input level increased. However, the response results were almost within the elastic range. The results of the SR model showed a similar trend but it was smaller than the result obtained from the 3D FE model. However, according to Fig. 19, low correlation was observed between the logarithm standard deviation (~0.2 or less) and the input level. Also, the results in the U–D direction were similar to those in the N–S direction. Therefore, in the following section, only the N–S direction responses were statistically analyzed.

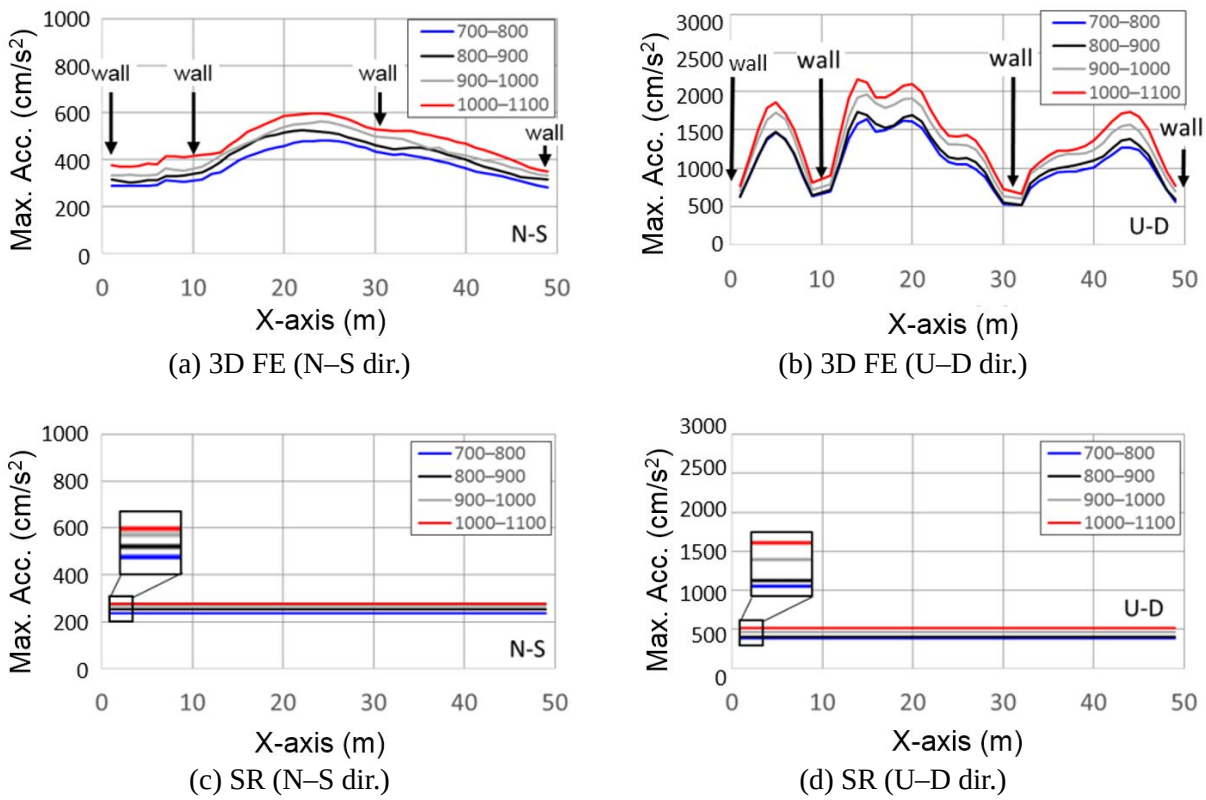

(a) 3D FE (N–S dir.)

(b) 3D FE (U–D dir.)

(c) SR (N–S dir.)

(d) SR (U–D dir.)

Fig. 18 Comparison of the median based on the input level (1F, Zone 1 (3D FE))

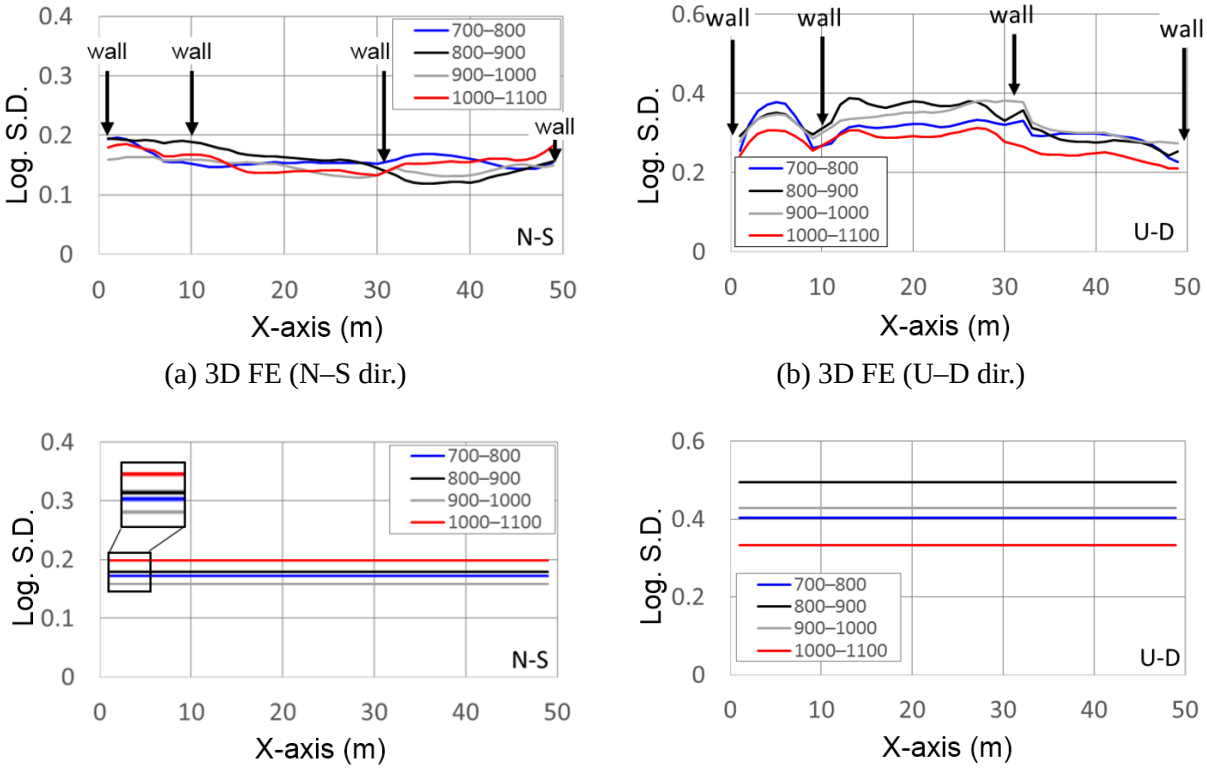

(a) 3D FE (N–S dir.)

(b) 3D FE (U–D dir.)

(c) SR (N–S dir.)

(d) SR (U–D dir.)

Fig. 19 Comparison of the variation based on the input level (1F, Zone 1 (3D FE))

4.3 Comparison Based on the Floor Height

To analyze the variation in responses based on the spatial position of the floor, the responses were analyzed as a function of the floor height (at a single floor position). The medians and the natural logarithm standard deviations for each of these profiles are depicted in Fig. 20. According to Fig. 20(a), the median of the 3D FE model was the lowest at B2F (TP of 22.7 m), and its maximum value was ~400 cm/s^2. In addition, the median for both B1F (TP of 29.7 m) and 1F (TP of 36.7 m) was larger than the corresponding value of B2F, and the maximum values were ~500 cm/s^2. However, the result of B1F was slightly smaller than the result of B2F in the result of the SR model. Further, these results are related with factors such as the thickness of the shear walls and the soil properties. On the other hand, according to Fig. 20(b), although the logarithm standard deviation of the 3D FE model was large near the opening at the 5-m position on the X-axis, the correlation between the variation and the floor height was small, with the variation remaining nearly constant at ~0.15 or less. In case of the SR model, there was a tendency that the variation increased with the floor height (in the range of ~0.14 to ~0.18).

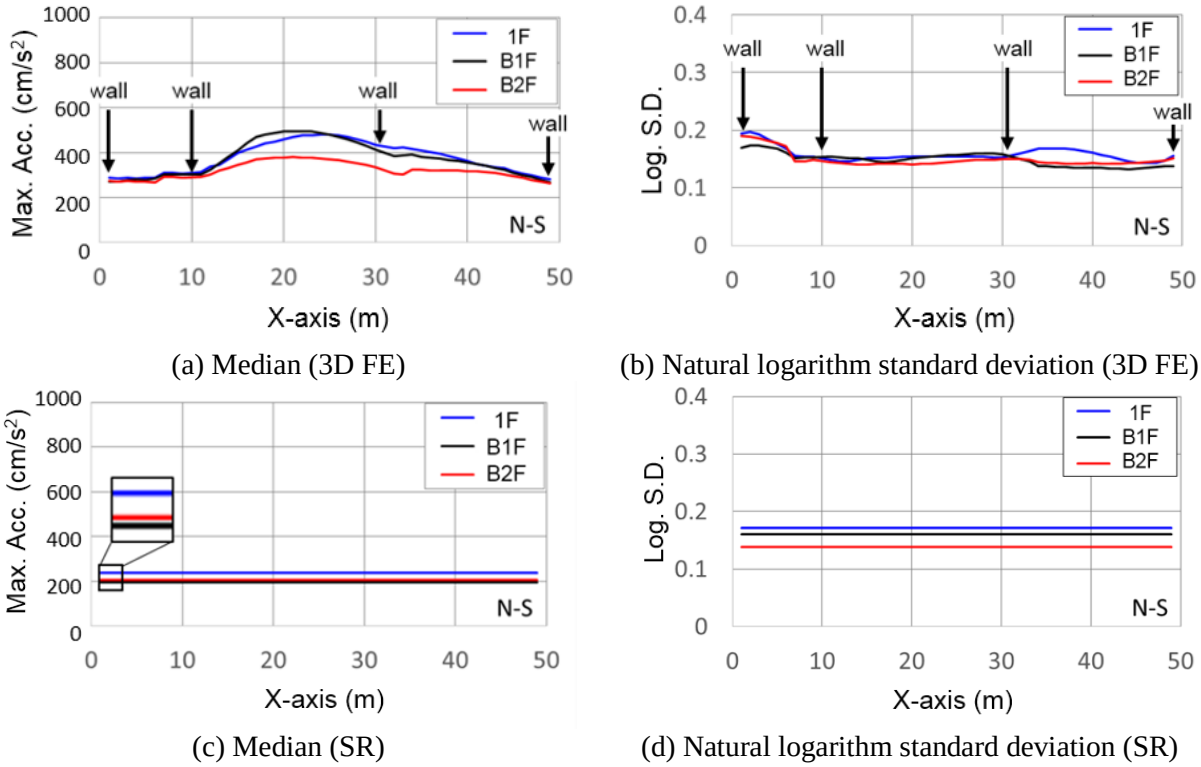

(a) Median (3D FE)

(b) Natural logarithm standard deviation (3D FE)

(c) Median (SR)

(d) Natural logarithm standard deviation (SR)

Fig. 20 Comparison based on the floor height (700–800 cm/s^2, Zone 1 (3D FE), N–S dir.)

4.4 Spatial Variation on the Floor Response Spectra of the 3D FE Model

In case of the conventional SR model, the spatial variation of the floor response on the same floor cannot be evaluated. In contrast, in the 3D FE model, the responses at various positions on the same floor can be evaluated. The authors focused on the floor response spectrum in the 3D FE model and evaluated its spatial variation. Figure 21 shows the output positions on the first floor. As an example, one HCGM wave of 700–800 cm/s^2 was used as the input ground motion (Fig. 22).

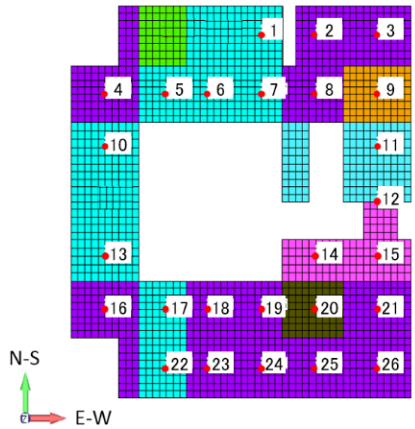

Fig. 21 Target floors of the reactor building (1F, 3D FE)

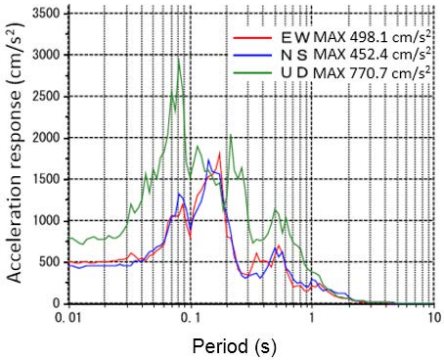

Fig. 22 Acceleration response spectrum of the input wave (h = 5%)

Figure 23 depicts the spatial variations of the floor acceleration response spectra (h = 5%) for each direction in various positions on the first floor. The response results are subjected to statistical analysis, and the median and natural logarithm standard deviation are depicted in Fig. 24. According to Fig. 24(a), the median of the dominant periods of floor response due to the difference in position on the same floor in the N–S and U–D direction was ~0.15 s. However, Fig. 24(b) shows that the natural logarithmic standard deviation tended to be large near a period of 0.1 s. In particular, a large variation in the U–D direction was observed at periods shorter than 0.1 s and was expected to have a large influence on the equipment.

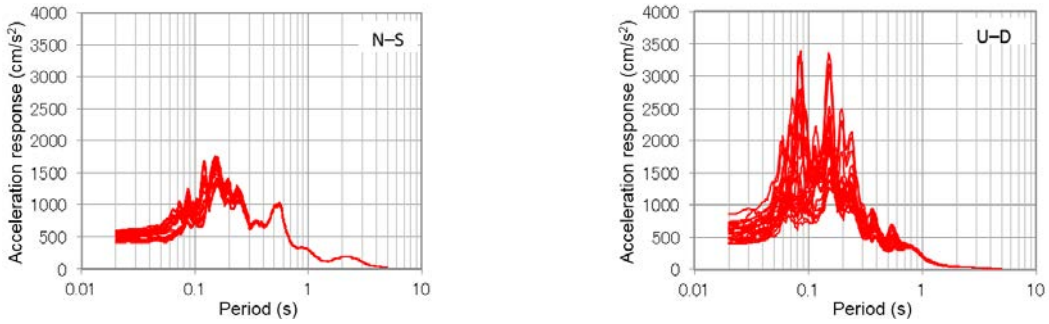

(a) N–S direction (b) U–D direction

Fig. 23 Spatial variation in case of the floor response spectra (h = 5%; 1F, 700–800 cm/s^2)

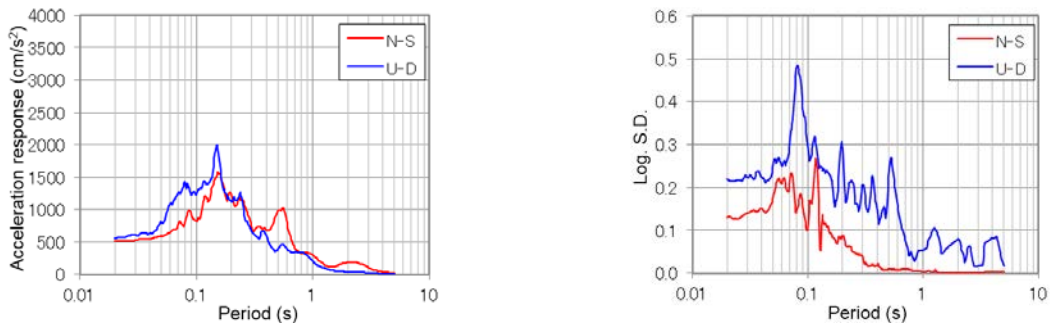

(a) Median (b) Natural logarithmic standard deviation

Fig. 24 Stochastic result of the floor response spectra (h = 5%; 1F, 700–800 cm/s^2)

5. DISCUSSION ON THE POTENTIAL USE OF RESULTS OF THIS STUDY IN SEISMIC PRA

The quantitative evaluation of the building response uncertainty in NPP seismic PRA is very important

because of the following reasons:

- Major uncertainty factor in a scenario directly linked with the core damage.
- Common uncertainty factor associated with the fragility of all the equipment in a building.

The epistemic uncertainty of building response analysis is estimated using an opinion extraction process involving multiple experts or engineering analysis of the seismic PRA. In either case, it is desirable to perform sensitivity analysis and probabilistic response analysis using the target plant data and include the analytical results based on the reference information for further engineering assessment.

In conventional SPRA, the SR model has been regarded as the basic model because it requires a relatively low calculation cost, has been verified well with the observation records, and yields conservative results most of the time. However, because the SR model is expressed by simplifying the three-dimensional structure, it includes errors associated with modeling. Therefore, it is necessary to confirm the influence of the differences in modeling by comparing the response results of detailed 3D FE modeling.

In this study, the authors found three-dimensional effects, such as out-of-plane deformation of walls and differences, due to the position of the same floor using the 3D FE model, which cannot be expressed using the SR model. The obtained knowledge could help the quantification of epistemic uncertainty in modeling of the seismic response analysis for SPRA.

6. CONCLUSIONS

A seismic response analysis for a 3D FE model and a conventional lumped mass with SR model for an NPP building was performed using 200 HCGM waves as the input. The variation of the maximum acceleration response of the NPP building was investigated to estimate the uncertainty related with different modeling methods. The following results were obtained.

- Based on the shear wall results, the difference in average responses between the two models was confirmed in the upper part of the building. The maximum response ratio was about 1.3, considered to be the influence of out-of-plane deformation. Also, this difference was confirmed in the middle part of the building because of the difference in the modeling method of the SSI effects. However, the variation difference based on the modeling methods was confirmed in the middle part of the building, and the response ratio was less than 0.8.

- The variation factor was classified as β_g and β_p. The former was almost constant (~0.20) regardless of the modeling method and the building height, whereas the latter tended to increase with the building height for the 3D FE model (~0.07 or less). Thus, the authors propose a maximum of 0.07 for β_p while using the SR model.

- Based on the floor results, the maximum acceleration response at the center part of the floor tended to be large, notably in the U–D direction. The maximum median values at the shear wall were small, and the corresponding values at the midpoints between each of the shear walls were large. In addition, the median result of the SR model tended to be smaller than that of the 3D FE model. The response ratio (3D FE/SR) on the 1F was ~1.6 for the N–S direction and ~2.5 for the U–D direction. However, the variation in case of the SR model was larger than that of the 3D FE model. The response ratio of variation on 1F was ~0.9 for the N–S direction and ~0.8 for the U–D direction.

- In this condition, the median of the maximum acceleration response increased as the input level increased regardless of the input direction and modeling method. However, a low correlation could be observed between the input level and the variation. The results of the SR model exhibited a similar trend.

- No clear correlation could be observed between the floor height and median responses because of factors such the thickness of the shear walls and the soil properties. However, the variation increased at positions near the opening, which cannot be discerned using a conventional SR model.

- Using the 3D FE model, the spatial variation of the floor response spectra for the same floor was investigated. The median of the dominant periods of floor response due to the difference in position on the same floor in the N–S horizontal and U–D vertical direction was ~0.15 s. However, a large variation was observed at periods shorter than 0.1 s, which was expected to have a large effect on the equipment.

In future studies, the authors intend to further examine the differences between modeling methods and the variation indices arising from the input ground motion periods. Also, a method will be examined to introduce the three-dimensional effect obtained in this study into fragility assessment. This will help to obtain a realistic response evaluation with respect to the SPRA for the NPP buildings.

REFERENCES

1) Atomic Energy Society of Japan: *A Standard for Procedure of Seismic Probabilistic Safety Assessment (PSA) for Nuclear Power Plants*, 2015. (in Japanese)
2) Takada, T., Itoi, T., Nishida A., Furuya, O. and Muramatsu, K.: Reliability Enhancement of Seismic Risk Assessment of NPP as Risk Management Fundamentals, Part II: Quantifying Epistemic Uncertainty in Fragility Assessment Using Expert Opinions, *Proc. SMiRT-23*, No.448, Manchester, UK, 2015.
3) Headquarters for earthquake research promotion: *Technical Report on National Seismic Hazard Maps for Japan*, 2009. (in Japanese)
4) Si, H. and Midorikawa, S.: New attenuation relationships for peak ground acceleration and velocity considering effects of fault type and site condition, *Journal of Structural and Construction Engineering (Transactions of AIJ)*, Vol. 64, No. 523, pp. 63–70, 1999. (in Japanese)
5) Nishida, A., Igarashi, S., Sakamoto, S., Uchiyama, Y., Yamamoto, Y., Muramatsu, K. and Takada, T.: Hazard-consistent ground motions generated with a stochastic fault-rupture model, *Nuclear Engineering and Design*, Vol. 295, pp. 875–886, 2015.
6) Choi, B., Nishida, A., Muramatsu, K. and Takada, T.: Uncertainty evaluation of seismic response of a nuclear facility using simulated input ground motions, *Proc. 12th Int. Conf. on Structural Safety and Reliability*, pp. 2206–2213, Vienna, Austria, 2017.
7) Choi, B., Nishida, A., Muramatsu, K. and Takada, T.: Uncertainty assessment of structural modeling in the seismic response analysis of nuclear facilities, *Proc. SMiRT-24*, No. 05-10-03, Busan, Korea, 2017.
8) Maekawa, K. and Fukuura, N.: Re-formulation of spatially averaged RC constitutive model with quasi-orthogonal bi-directional cracking, *Journal of Materials, Concrete Structures and Pavements, JSCE*, No. 634/V-45, pp. 157–176, 1999. (in Japanese)
9) Nishida, A., Iigaki, K., Sawa, K. and Li, Y.: Influence of Differences Between Seismic Safety Evaluation Methods for Equipment and Piping of a Nuclear Facility, *Proc. PVP2015*, No. 45913, Boston, USA, 2015.
10) Choi, B., Nishida, A. and Nakajima, N.: A Sensitivity analysis for construction of the seismic response analysis model of a nuclear reactor building by using a three-dimensional finite element model, *Journal of Structural Engineering*, Vol. 63B, pp. 325–333, 2017. (in Japanese)

(Submitted: June 1, 2018)
(Accepted: September 7, 2019)